Pressure-induced strong adhesion between chitosan nanofilms

Tan Qiyan   Kan Yajing   Zhao Gutian   Qiu Yinghua   Chen Yunfei

(School of Mechanical Engineering, Southeast University, Nanjing 211189, China)

(Jiangsu Key Laboratory for Design and Manufacture of Micro-Nano Biomedical Instruments, Nanjing 211189, China)

Abstract: The surface and adhesion forces between chitosan-coated mica surfaces in an acetic acid buffer solution were measured using a surface force apparatus (SFA). The force-distance profiles were obtained under different pressure conditions. It was found that the chitosan was adsorbed on the mica surface and formed a stable nanofilm under acid conditions. The adsorbed chitosan nanofilms induced a short-range monotonically steric force when two such surfaces came close in the acid buffer. The adhesion forces between the two chitosan-coated mica surfaces varied with the loads. Strong adhesion between the two chitosan-coated mica surfaces was observed at high pressure. Such pressure-dependent adhesion properties are most likely related to the molecular configurations and hydrogen bonds reordering under high confinement.

Key words: surface force apparatus (SFA); chitosan; adhesion; pressure; mica surface

doi: 10. 3969/j. issn. 1003 − 7985. 2015. 01. 019

C hitosan, the only cationic biopolymer originating from natural sources, is a linear polysaccharide composed of β (1-4) glucosamine and N-acetyl glucosamine monomers[1]. It is the N-deacetylated derivative of its parent biopolymer chitin, a naturally abundant mucopolysaccharide and the supporting material of crustaceans and insects[2]. Chitin's poor solubility in aqueous solution or organic solvents is the major limiting factor in its practical applications. A few applications of chitin or modified chitins, e. g. as a raw material for man-made fibers[3], have been reported. Conversely, chitosan is soluble in a slightly acidic solution and is more suitable for useful applications. Chitosan has been extensively studied in the pharmaceutical industry[4], due to its excellent biodegradable and admirable biocompatible characteristics. In addition, chitosan has attracted much attention as a functional material in many fields, such as food science[5], the cosmetics industry[6], water treatment[7], and agriculture[8].

The structural and physiochemical properties of chitosan in solution depend largely on molecular weight, the degree of deacetylation, pH, and ionic strength[9]. Chitosan is completely soluble and behaves as a weak cationic polyelectrolyte below pH 6, at which most of its amino groups are protonated. Many studies have been performed to elucidate the properties of adsorbed chitosan on mineral and metal oxide surfaces[9−16]. The solid surface properties, such as surface charge, can be changed by the absorption of weak cationic chitosan layers[15]. The pH dependence of interaction forces between adsorbed chitosan layers was investigated by a surface force apparatus (SFA)[9]. The weak friction force between mica surfaces bearing chitosan under low pressures was found by Kampf et al[16]. They attributed it to the weak interpenetration and hydration sheaths of charge chitosan together with counterion osmotic pressure. Atomic force microscopy (AFM) was used to study the absorption and desorption of individual chitosan polymer chains from substrates with a varying chemical composition[12−13]. Chitosan adsorbed onto a flat substrate shows elongated single strands or aggregated bundles. The desorption energies were dependent on the affinity of chitosan to the solid substrates. Recently, a stable, rigid and thin adsorption monolayers chitosan on a silica surface was observed under a wide range of conditions[10]. It is found that the strong adhesion and cohesion of chitosan were dependent on pH[11], which is largely different from the previous results[9].

Due to the complexity and flexibility of chitosan, the molecule configurations vary under different conditions, such as pressure and temperature. However, exploring the molecular mechanisms of interactions between chitosan nanofilms under different pressures remains rather limited. In the present study, we investigate the interactions of chitosan adsorbed on mica surfaces in aqueous solution. In particular, we focus on the roles of pressure on the adhesion and structural properties of the adsorbed chitosan layer. We find that the strong adhesion can be obtained under high pressure conditions. Our results can provide important information for understanding the adhesion mechanism of adsorbed chitosan monolayers.

1 Experimental Methods

1.1 Force measurements

The interaction forces between chitosan-coated mica

---

surfaces were investigated by the SFA 2000 system from SURFORCE, LLC at Santa Barbara[17]. SFA has been widely used to measure the intermolecular and surface forces in various fields with 10 nN force sensitivity and 0. 1 nm distance resolution. The surfaces were visualized by using a video camera to record the optical multiple beam interferometry (MBI) fringes known as fringes of equal chromatic order (FECO), which allow the surface shape, contact radius r, area $A = \pi r^2$, and film thickness D to be measured. The detailed description of the SFA 2000 system can be found in Refs. [18 − 20]. The experimental setup in this study is shown in Fig. 1.
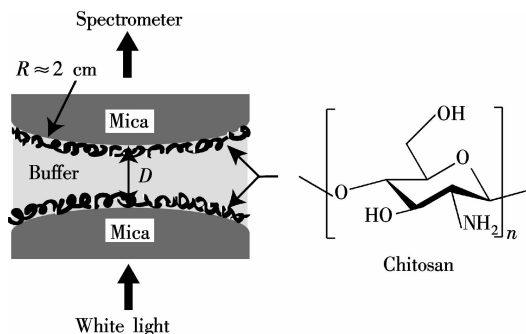

Fig. 1 The schematic of the experimental setup

1. 2   Materials

Chitosan (low molecular weight, product number 448869) was purchased from Sigma-Aldrich, the detailed structure of which is shown in Fig. 1. According to the manufacturer, the degree of deacetylation of chitosan was more than 75. 0%. A chitosan solution (10 μg/mL) was prepared by dissolving chitosan powder in 100 mmol/L acetic acid (from Sigma-Aldrich) solution (pH 3. 2). The solution was then stirred gently for at least 4 h at room temperature. High purity water with a resistivity of 18. 25 MΩ · cm was taken from a water purification system. All chemicals were used as received.

1. 3   Surface preparations

Atomically smooth mica surfaces (Grade 1, S&J Trading, Inc.) with a thickness of about 3 μm were manually cleaved in a laminar flow cabinet. A uniform silver film of 50 nm thickness was coated on the mica surface in a physical vapor deposition system. Two back-silvered mica surfaces were then glued onto cylindrical silica disks (Radius R is about 2 cm) by using Epoxy Resin ("EPON 1004F", Shell Chemicals). The mica-coated disks were mounted in the SFA facing each other in a crossed-cylinder configuration, equivalent to the geometry of a sphere over a flat substrate. The zero separation ($D = 0$) was set as the adhesive contact between two bare mica surfaces in a dry nitrogen atmosphere. After calibration, the mica surfaces were immersed into 10 μg/mL chitosan solution for 20 min. Then, the mica surfaces

were rinsed thoroughly with 100 mmol/L acetic acid buffer (pH = 3. 2) to remove the free chitosan. Immediately, the chitosan-coated mica surfaces were mounted into the SFA chamber. A drop of 100 mmol/L acetic acid buffer (pH = 3. 2) was injected into the gap between the mica surfaces. The chamber was sealed and the whole system was maintained until reaching equilibrium. Then, the force-distance profiles were measured at different pressures with an approaching speed of (4 ± 1) nm/s. During the experiments, the chamber was saturated with water vapor. All the experimental data shown here was reproducibly repeated two or more times.

1. 4   AFM

Topographical images of adsorbed chitosan nanofilms were obtained using AFM under 100 mmol/L acetic acid buffer conditions. A freshly cleaved mica surface was first dipped into a 10 μg/mL chitosan solution for 20 min followed by being rinsed thoroughly with a 100 mmol/L acetic acid buffer (pH = 3. 2). Images were obtained by scanning the sample with an AFM operated in tapping mode at room temperature.

2   Results and Discussion

Chitosan became positively charged under slightly acidic conditions, due to the protonation of the amino groups. The electrostatic attraction is the main driving force of the adsorption of chitosan to negatively charged mica in a 100 mmol/L acetic acid buffer (pH = 3. 2). In previous studies[12], the adsorbed chitosan films were observed to be relatively smooth and to have a flat conformation. AFM images of chitosan under liquid showed the presence of sparse or entangled elongated strands. Stable and flat chitosan was adsorbed on the mica surface. The roughness of adsorbed chitosan is less than 0. 4 nm, as shown in Fig. 2.
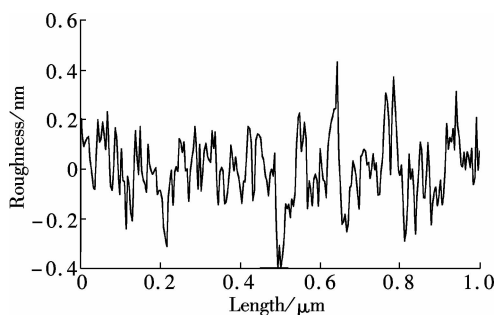

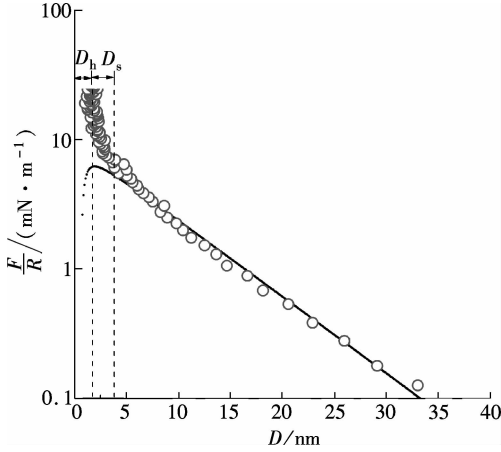**Fig. 2**   AFM image of the roughness of adsorbed chitosan on mica

We used the SFA 2000, at room temperature (22 ± 0. 1)℃, to measure the surface forces as a function of surface separation between two chitosan-coated mica surfaces in a 100 mmol/L acetic acid buffer solution (pH = 3. 2). Fig. 3 shows the results of one pair of mica surfaces. The forces F are normalized by the radius R of the

curved mica surface. The value F/R is equal to $2\pi E$ based on the Derjaguin approximation, where E is the corresponding surface energy per unit area for two flat parallel surfaces. The long-range repulsive forces, starting at about (32 ± 1) nm, were observed from three different experiments, which can be attributed to the repulsive electrostatic double-layer forces. The range of force is in agreement with the previous report[11], but shorter than that reported by Claesson[9], which may be induced by the difference of buffer solutions.

Fig. 3   The surface forces F/R between two chitosan-coated mica surfaces

To interpret this phenomenon, we compare our experimental data with the DLVO theoretical predictions, by summing electrostatic double-layer forces and Van der Waals forces. Taking acetic acid as a 1:1 electrolyte solution[9], the surface force profiles can be fitted to the DLVO theoretical calculations for a monovalent electrolyte solution, given by

$$\frac{F}{R} = 128\pi\rho_b k_B T\kappa^{-1}\tanh^2\left(\frac{e\phi_0}{4k_B T}\right)e^{-\kappa D} - \frac{A}{12\pi D^2} \quad (1)$$

where ρ_b is the bulk salt concentration; k_B is the Boltzmann constant; T is the temperature; ϕ_0 is the effective surface potential; e is the electronic charge; A is the Hamaker constant of mica across water, 2×10^{-20} J; D is the surface separation; κ^{-1} is the Debye screening length. The Debye screening length for 1:1 electrolyte solution can be given by
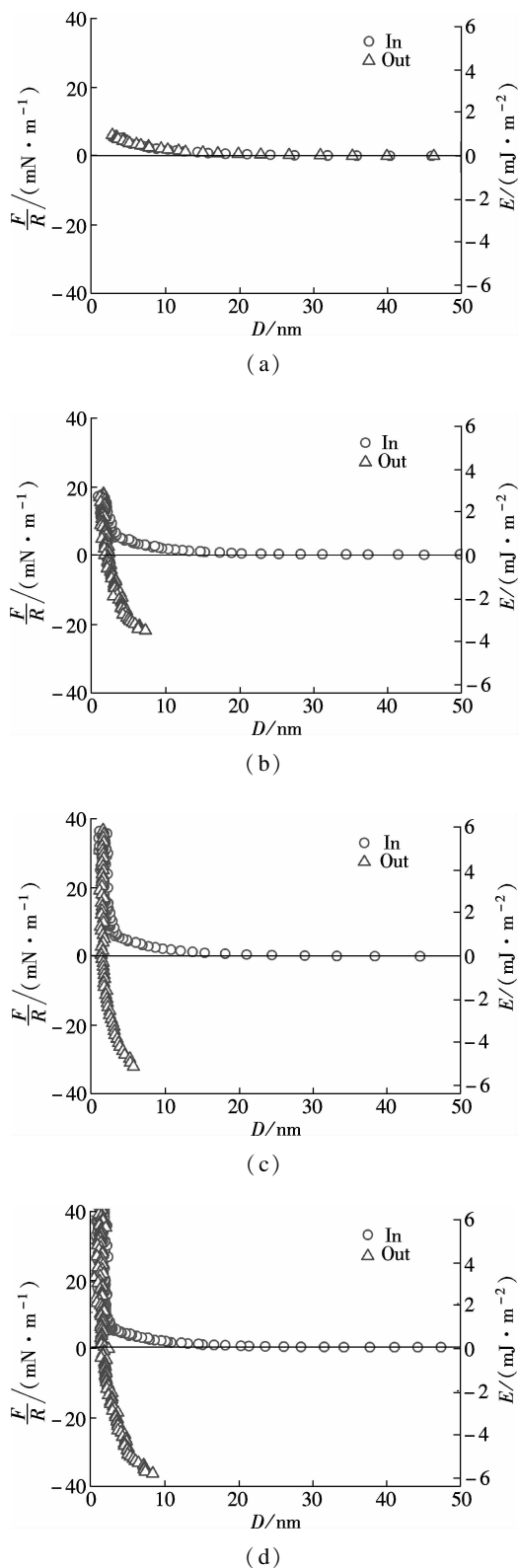
$$\kappa^{-1} = \left(\frac{\varepsilon\varepsilon_0 k_B T}{2\rho_b e^2}\right)^{1/2} \quad (2)$$

where $\varepsilon\varepsilon_0 = 80$ is the dielectric constant. The solid line in Fig. 3 shows that the measured surface forces agree well with the theoretical calculations, which gives a fitted Debye length of 7.37 nm and an effective surface potential of 134 mV. The corresponding bulk salt concentration 17 mmol/L can be obtained by Eq. (2). The surface charge of mica surfaces has changed the sign from negative to positive, due to the absorption of positively charged chi-

tosan. The long-range repulsive electrostatic double-layer force dominates down to $D_s = (3.4 \pm 0.1)$ nm. The short-range repulsive steric force is stronger than the attractive Van der Waals force predicted from the DLVO models below D_s. The adsorption of chitosan to mica was confirmed by the increase in the short-range steric force. The repulsive steric force started around $D > 4$ nm on the approach process, which indicated that initially, the adsorbed chitosan was in an exposing loops structure. With the increasing compression load, the exposing loops chitosan became a flatter configuration. The mica surfaces can be compressed together and finally contacted flatly at a "hard wall" distance $D_h = (1.4 \pm 0.1)$ nm. The "hard wall" distance in this study is defined as the mica-mica separation distance. The thickness of the adsorbed chitosan layer on mica was determined to be half of the "hard wall" distance. Here, the adsorbed chitosan thickness is about (0.7 ± 0.1) nm per surface. The adsorbed chitosan layer is slightly thicker than the reported thickness of 0.5 nm on silica substrate[10].

The measured surface and adhesion forces between two chitosan-coated mica surfaces under different compression loads are presented in Fig. 4. The circle and triangle symbols in Fig. 4 are the approach (in) and separation (out) processes, respectively. The chitosan-coated mica surfaces were first driven into contact at a separation of $D_h = (3.2 \pm 0.1)$ nm, then stopped and separated immediately, as shown in Fig. 4(a). The detected force was the only repulsive double-layer force, and no short-range steric force was observed. The maximum repulsion force was about 6 mN/m, indicating that the interaction energy of chitosan layers is approximately 1 mJ/m² based on the Derjaguin approximation. Under these conditions, the adsorbed chitosan layer is still in exposing loops or the swollen structure. The surfaces were not flattened and the pressure can be ignored. The adsorbed chitosan layers are slightly interpenetrated at a separation of $D_h = (3.2 \pm 0.1)$ nm. We reasoned that the molecules adsorbed to the surfaces would act as adhesive bridges when the surfaces were separated. However, no adhesion was measured between the two chitosan-coated mica surfaces. The pull-off force (or adhesion force) to separate the two mica surfaces is zero.

The force profile varies greatly with the increasing load, as shown in Fig. 4(b). When the load increased to 17.5 mN/m, a short-range steric force emerged and the "hard wall" decreased to $D_h = (1.5 \pm 0.1)$ nm. These measurements indicate that the adsorbed chitosan layer would be in a flat conformation under confinement. The steric force was induced by the compression of the exposing structure of the adsorbed chitosan layer. The adhesion force increased dramatically with load. The pull-off force was up to 21.1 mN/m. The corresponding adhesion energy of the adsorbed chitosan layer was about 3.4 mJ/
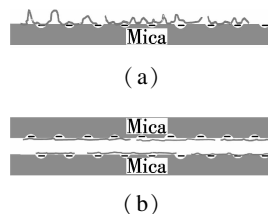
(a)

(b)

(c)

(d)

Fig. 4 The surface and adhesion forces between two chitosan-coated mica surfaces at different compression loads. (a) The maximum load $F/R = 6$ mN/m; (b) The maximum load $F/R = 17.5$ mN/m; (c) The maximum load $F/R = 36.6$ mN/m; (d) The maximum load $F/R = 41.2$ mN/m

m^2. When the load reached 36.6 and 41.2 mN/m, the hard wall was reduced to $D_h = (1.4 \pm 0.1)$ nm. The steric force coincides with that at low loads. However, under this compressive load, the diameter of surfaces flattened area was about 40 μm when the load was increased to $F/R \approx 40$ mN/m. The pressure in the contact area can be calculated by $P = F/A \approx 0.6$ MPa. The maximum adhesion force of 36.4 mN/m was observed as the compressing load achieved about 40 mN/m. Even the load was up to 100 mN/m (not shown here), the last two adsorbed chitosan layers cannot be squeezed and the adhesion cannot exceed the maximum adhesion force measured above.

The initially adsorbed chitosan may be in an exposing loop structure even if the roughness is less than 0.4 nm. Fig. 5 shows that the configuration and loop structure of chitosan are changed due to the confinement under load. The measured strong adhesion of chitosan layers under high pressure in an acetic acid buffer is comparable with that of mussel foot protein[21], which is an adhesive protein that can achieve strong and durable attachments to a variety of surfaces. This measured adhesion, achieved by compressing the chitosan films, is likely to be due to hydrogen bonds originating from the moieties in the chitosan molecule, which interacts with each other and with mica surfaces. The configuration and hydrogen bonds of chitosan layers are altered under high pressure. The hydrogen bonds have been considered to be the main driving force of strong adhesion induced by other proteins[21] or the polyelectrolytes. When the hydrogen bonds between the chitosan nanofilms are formed, it is difficult to change the configurations with the increase in the compression load between chitosan films.

(a)

(b)

Fig. 5 The configuration of adsorbed chitosan. (a) Initially adsorbed chitosan; (b) Flatted chitosan layer under high pressure confinement

3 Conclusion

This study demonstrates that the configuration and adhesion of adsorbed chitosan layers on mica surfaces are strongly influenced by the compression load. Chitosan can be adsorbed on the mica surface in an acetic acid buffer through electrostatic interaction. The adsorption of the chitosan layer changed the surface charge of mica surface from negative to positive. The adhesion forces between two chitosan-coated mica surfaces varied with approaching load. The initially adsorbed chitosan molecules reoriented their configuration confined between two mica surfaces under different pressures. High pressure between two such surfaces can induce strong adhesion due to molecular configurations and hydrogen bonds reordering. We anticipate that this study will contribute to understanding

the properties of polymer and polyelectrolytes under confinement.

References

[1] Dash M, Chiellini F, Ottenbrite R M, et al. Chitosan—a versatile semi-synthetic polymer in biomedical applications[J]. *Progress in Polymer Science*, 2011, **36**(8): 981 – 1014.

[2] Sashiwa H, Aiba S. Chemically modified chitin and chitosan as biomaterials[J]. *Progress in Polymer Science*, 2004, **29**(9): 887 – 908.

[3] Kumar M N V R. A review of chitin and chitosan applications[J]. *Reactive & Functional Polymers*, 2000, **46**(1): 1 – 27.

[4] Shu X Z, Zhu K J. The influence of multivalent phosphate structure on the properties of ionically cross-linked chitosan films for controlled drug release[J]. *European Journal of Pharmaceutics and Biopharmaceutics*, 2002, **54**(2): 235 – 243.

[5] Rinaudo M. Chitin and chitosan: properties and applications[J]. *Progress in Polymer Science*, 2006, **31**(7): 603 – 632.

[6] Yi H, Wu L Q, Bentley W E, et al. Biofabrication with chitosan[J]. *Biomacromolecules*, 2005, **6**(6): 2881 – 2894.

[7] Ngah W S W, Teong L C, Hanafiah M A K M. Adsorption of dyes and heavy metal ions by chitosan composites: a review[J]. *Carbohydrate Polymers*, 2011, **83**(4): 1446 – 1456.

[8] Domard A. A perspective on 30 years research on chitin and chitosan[J]. *Carbohydrate Polymers*, 2011, **84**(2): 696 – 703.

[9] Claesson P M, Ninham B W. pH-dependent interactions between adsorbed chitosan layers[J]. *Langmuir*, 1992, **8**(5): 1406 – 1412.

[10] Tiraferri A, Maroni P, Caro R D, et al. Mechanism of chitosan adsorption on silica from aqueous solutions[J]. *Langmuir*, 2014, **30**(17): 4980 – 4988.

[11] Lee D W, Lim C, Israelachvili J N, et al. Strong adhesion and cohesion of chitosan in aqueous solutions[J]. *Langmuir*, 2013, **29**(46): 14222 – 14229.

[12] Khokhlova M A, Gallyamov M O, Khokhlov A R. Chitosan nanostructures deposited from solutions in carbonic acid on a model substrate as resolved by AFM[J]. *Colloid and Polymer Science*, 2012, **290**(15): 1471 – 1480.

[13] Kocun M, Grandbois M, Cuccia L A. Single molecule atomic force microscopy and force spectroscopy of chitosan[J]. *Colloids and Surfaces B: Biointerfaces*, 2011, **82**(2): 470 – 476.

[14] Guibal E. Interactions of metal ions with chitosan-based sorbents: a review[J]. *Separation and Purification Technology*, 2004, **38**(1): 43 – 74.

[15] Kampf N, Ben-Yaakov D, Andelman D, et al. Direct measurement of sub-debye-length attraction between oppositely charged surfaces[J]. *Physical Review Letters*, 2009, **103**(11): 118304.

[16] Kampf N, Raviv U, Klein J. Normal and shear forces between adsorbed and gelled layers of chitosan, a naturally occurring cationic polyelectrolyte[J]. *Macromolecules*, 2004, **37**(3): 1134 – 1142.

[17] Israelachvili J N. *Intermolecular and surface forces*[M]. New York: Elsevier Science, 2011:240.

[18] Zhao G T, Guo W C, Tan Q Y, et al. Force measurement between mica surfaces in electrolyte solutions[J]. *Journal of Southeast University: English Edition*, 2013, **29**(1): 57 – 61.

[19] Zhao G T, Tan Q Y, Xiang L, et al. Imaging the condensation and evaporation of molecularly thin ethanol films with surface forces apparatus[J]. *Review of Scientific Instruments*, 2014, **85**(1): 013702.

[20] Tan Q Y, Zhao G T, Qiu Y H, et al. Experimental observation of the ion-ion correlation effects on charge inversion and strong adhesion between mica surfaces in aqueous electrolyte solutions[J]. *Langmuir*, 2014, **30**(36): 10845 – 10854.

[21] Yu J, Kan Y, Rapp M, et al. Adaptive hydrophobic and hydrophilic interactions of mussel foot proteins with organic thin films[J]. *Proceedings of the National Academy of Sciences*, 2013, **110**(39): 15680 – 15685.

压力诱导的壳聚糖纳米薄膜层间的强黏附作用

谭启檐   阚亚鲸   赵古田   裘英华   陈云飞

（东南大学机械工程学院，南京 211189）

（江苏省微纳生物医疗器械设计与制造重点实验室，南京 211189）

摘要: 利用表面力仪测量了在醋酸缓冲液中吸附壳聚糖的云母表面间表面力和黏附力，并获得了不同压力条件下的力–距离特性曲线. 结果表明:在酸性环境下，壳聚糖能够吸附到云母表面并形成一层稳定的纳米薄膜层. 当两云母表面相互靠近时，吸附壳聚糖纳米层会引起短程单调空间位阻力. 两吸附壳聚糖的云母间黏附力随着载荷的变化而变化. 在较大压力条件下，两吸附壳聚糖的云母表面间呈现很强的黏附作用. 这种随压力变化的黏附特性主要是由于在高度受限环境下分子结构和氢键的重新排序所致.

关键词: 表面力仪;壳聚糖;黏附;压力;云母表面

中图分类号: O631.1